Neurobiology of Disease 42 (2011) 231–241

Contents lists available at ScienceDirect

Neurobiology of Disease

journal homepage: www.elsevier.com/locate/ynbdi

High-frequency (80–500 Hz) oscillations and epileptogenesis in temporal lobe epilepsy

Maxime Lévesque [a], Aleksandra Bortel [a], Jean Gotman [a], Massimo Avoli [a,b,*]

[a] Montreal Neurological Institute and Department of Neurology & Neurosurgery, McGill University, 3801 University Street, Montreal, Qc, Canada H3A 2B4
[b] Dipartimento di Medicina Sperimentale, Sapienza Università di Roma, Viale del Castro Laurenziano 9, 00185 Roma, Italy

ARTICLE INFO

Article history:
Received 17 September 2010
Revised 17 November 2010
Accepted 2 January 2011
Available online 14 January 2011

Keywords:
High frequency oscillations
Fast ripples
Ripples
Interictal spikes
Epileptogenesis
Pilocarpine

ABSTRACT

High-frequency oscillations (HFOs), termed ripples (80–200 Hz) and fast ripples (250–600 Hz), are recorded in the EEG of epileptic patients and in animal epilepsy models; HFOs are thought to reflect pathological activity and seizure onset zones. Here, we analyzed the temporal and spatial evolution of interictal spikes with and without HFOs in the rat pilocarpine model of temporal lobe epilepsy. Depth electrode recordings from dentate gyrus (DG), CA3 region, subiculum and entorhinal cortex (EC), were obtained from rats between the 4th and 15th day after a *status epilepticus* (SE) induced by i.p. injection of pilocarpine. The first seizure occurred 6.1 ± 2.5 days after SE (n = 7 rats). Five of 7 animals exhibited interictal spikes that co-occurred with fast ripples accounting for 4.9 ± 4.6% of all analyzed interictal spikes (n = 12,886) while all rats showed interictal spikes co-occurring with ripples, accounting for 14.3 ± 3.4% of all events. Increased rates of interictal spikes without HFOs in the EC predicted upcoming seizures on the following day, while rates of interictal spikes with fast ripples in CA3 reflected periods of high seizure occurrence. Finally, interictal spikes co-occurring with ripples did not show any specific relation to seizure occurrence. Our findings identify different temporal and spatial developmental patterns for the rates of interictal spikes with or without HFOs in relation with seizure occurrence. These distinct categories of interictal spikes point at dynamic processes that should bring neuronal networks close to seizure generation.

© 2011 Elsevier Inc. All rights reserved.

Introduction

High frequency oscillations (HFOs) – which include ripples: 80–200 Hz, and fast ripples: 250–600 Hz – can be recorded from the hippocampus, entorhinal cortex (EC) and neocortex of patients with intractable focal epilepsy and in animals made epileptic by experimental procedures (Bragin et al., 1999, 2002a, 2003, 2004, 2007; Jacobs et al., 2008; Staba et al., 2007). HFOs are mainly related to interictal spikes and are state-dependent since they occur more frequently during slow-wave sleep (Bagshaw et al., 2009; Bragin et al., 2000; Staba et al., 2004). Higher HFO rates are significantly correlated with higher seizure frequency in epileptic patients (Ziljmans et al., 2009), and appear to be more specific markers than interictal spikes in identifying the seizure onset zone, independently of the underlying pathology (Crépon et al., 2010; Jacobs et al., 2008; 2009). Moreover, the spatial distribution of HFOs in the epileptogenic zone depends on the type of epileptic discharge, as widespread interictal spikes propagating across multiple cortical regions are often related to HFOs that can be recorded on multiple channels (Schevon et al., 2009).

These findings indicate that HFOs may mirror pathologic mechanisms that occur during chronic epilepsy. However, their role during the epileptogenic process is still unclear. Studies in rodents have shown that HFOs may reflect epileptogenesis since they are recorded in the dentate gyrus (DG) many days before the onset of spontaneous seizures induced by kainic acid, and only in animals that will later develop seizures (Bragin et al., 2004). Moreover, the latent period is shorter and the rate of spontaneous seizures is higher in animals in which HFOs occurred shortly after kainic acid injection (Bragin et al., 2004). These results thus support the hypothesis conceiving HFOs as a marker of abnormal neuronal network activity.

The spatial and temporal patterns of HFO development in different limbic areas as well as their relation to spontaneous seizures following an initial SE is, however, poorly defined in animal models of temporal lobe epilepsy (TLE). Hence, we used the pilocarpine model of TLE and performed chronic recordings in the entorhinal cortex (EC), DG, CA3 region and subiculum to answer the following questions: (i) how does the spatial distribution and the temporal evolution of interictal spikes with and without HFOs relate to rates of spontaneous seizures and (ii) are there limbic areas showing HFO activity that correlate more than others with the occurrence of spontaneous seizures over time. We hypothesized that HFOs mirror the evolutionary state of the epileptogenic tissue and that the relation to seizure occurrence will reveal pathologic activity from regions that bring neural networks close to seizure onset.

* Corresponding author. Montreal Neurological Institute, McGill University, 3801 University Street, Montreal, PQ, Canada H3A 2B4. Fax: +1 514 398 8106.
E-mail address: massimo.avoli@mcgill.ca (M. Avoli).
Available online on ScienceDirect (www.sciencedirect.com).

0969-9961/$ – see front matter © 2011 Elsevier Inc. All rights reserved.
doi:10.1016/j.nbd.2011.01.007

Materials and methods

Animal preparation

Sprague–Dawley rats (250–300 g) were obtained from Charles River Laboratories (St-Constant, Qc, Canada), and let habituate for 72 hours after delivery before pilocarpine treatment. They were housed under controlled environmental conditions, at 22 (±2) °C and 12 h light/12 h dark cycle (lights on from 7:00 a.m. to 7:00 p.m.) with food and water *ad libitum*. All procedures were approved by the Canadian Council of Animal Care and all efforts were made to minimize the number of animals used and their suffering.

Rats were injected with scopolamine methylnitrate (1 mg/kg i.p.; Sigma-Aldrich, Canada) and 30 min later with a single dose of pilocarpine hydrochloride (380 mg/kg, i.p.; Sigma-Aldrich, Canada). Their behavior was scored according to the Racine scale (Racine, 1972), and SE was defined as continuous stage 5 seizures. Rats that did not show SE after 30 min were administered with additional half doses of pilocarpine (190 mg/kg, i.p.). SE was terminated after 1 h by injection of diazepam (5 mg/kg, i.p.; CDMV, Canada) and ketamine (50 mg/kg, i.p.; CDMV, Canada) (Martin and Kapur, 2008). The mortality rate was 13%, and the surviving animals were allowed to recover for 72 h before surgery.

Rats were anaesthetized with isoflurane (3%) in 100% O_2. They were then positioned in a stereotaxic frame so that lambda and bregma layed in the same horizontal plane. An incision was made in the skin to expose the skull plate. Four stainless steel screws (2.4 mm length) were fixed to the skull and up to 4 small holes were drilled to allow the implantation of bipolar electrodes (20–30 kΩ, 30–50 mm length, distance between exposed tips: 500 μm) made by gluing two insulated copper wires. Electrodes were implanted in the CA3 region of the ventral hippocampus (AP: −4.4, ML: ±4, DV: −8.8), medial EC (AP: −6.6, ML: ±4, DV: −8.8), ventral subiculum (AP: −6.8, ML: ±4, DV: −6) and DG (AP: −4.4, ML: ±2.4, DV: 3.4) (Supplementary Fig. 1A). Screws and electrode pins were connected with a pin connector and fastened to the skull with dental cement. A cortical screw placed in the frontal bone was used as the reference, and a second screw, placed on the opposite side of the frontal region, was used as the ground (Supplementary Fig. 1B). After surgery, animals received topic application of Chloramphenicol (Erfa, Canada) and Lidocain (5%; Odan, Canada) and were injected with Ketoprofen (5 mg/kg s.c.; Merail, Canada), Buprenorphine (0.01–0.05 mg/kg s.c. repeated every 12 h if necessary; CDMV, Canada) and 2 ml of 0.9% sterile saline (s.c.).

Local field potential recordings and histological localization of depth electrodes

After surgery, rats were housed individually in custom-made Plexiglas boxes (30×30×40 cm) and let habituate to the environment for 24 h. The pin connector was then connected to multichannel cables and electrical swivels (Slip ring T13EEG, Air Precision, France; or Commutator SL 18 C, HRS Scientific, Canada) and continuous local field potential (LFP)-video monitoring (24 hour per day) was performed. LFP signals were amplified via an interface kit (Mobile 36ch LTM ProAmp, Stellate, Montreal, QC, Canada), and sampled at 2 kHz per channel. Infrared cameras were used to record day/night video files that were time-stamped for integration with the electrophysiological data using monitoring software (Harmonie, Stellate, Montreal, QC, Canada). Throughout the recordings, animals were placed under controlled conditions (22±2 °C, 12-hour light/dark schedule) and provided with food and water *ad libitum*. LFP-video recording was performed up to 15 days after SE.

At the end of the recording period, rats were deeply anaesthetized with isoflurane and electrode localization was aided by lesioning the surrounding tissue by passing current (500 μA, 120 s) through each recording electrode. Rats were maintained under deep anaesthesia with isoflurane and decapitated. Brains were extracted and post-fixed with formaldehyde (BioLynx Inc, Canada) for at least 48 hours and later placed in a 30% sucrose-formalin solution for another 48 hours. They were then frozen in pulverized dry ice and subsequently sliced (30 μm-thick) using a cryostat. Brain sections were mounted on gelatinized glass slides and stained using a Cresyl Violet solution. Location of the lesions was evaluated according to Paxinos and Watson (1998) (Supplementary Fig. 1C).

Detection of high-frequency oscillatory events

Periods of slow-wave sleep – defined by muscular atonia (curled body position) and delta activity (1–6 Hz) – were selected for behavioural and LFP analysis since HFOs are more prominent during this sleep state (Bagshaw et al., 2009; Staba et al., 2004). In each rat, one artefact-free period of slow-wave sleep lasting 10 min was selected for each day and for each region. These time-periods were then exported to Matlab 7.9.0 (Mathworks, Natick, MA) using custom-built routines, and analyzed off-line. In order to prevent a post- or pre-seizure effect on HFO rates, time-periods were selected only if they were preceded and followed by a seizure-free period of at least 1 h. For each 10-minute period, raw LFP recordings were band-pass filtered in the 80–200 Hz and in the 250–600 Hz frequency range using an FIR filter; zero-phase digital filtering was used to avoid phase distortion.

A multi-parametric algorithm was employed to identify oscillations in each frequency range, using routines based on standardized functions (Signal Processing Toolbox). In order to be considered as a potential HFO candidate, oscillatory events in each frequency band had to show at least three consecutive cycles that crossed a standard threshold (3 SDs above the background mean). Moreover, the time lag between two consecutive cycles in the ripple frequency range had to be between 5 and 12.5 ms for ripples, and between 1.6 and 4 ms for fast ripples. Oscillations in the ripple frequency range were only kept for further analysis if they did not co-occur with a fast ripple, in order to exclude false positives that may have represented either an effect of filtering very fast spikes or an effect of movement artefacts. Similarly, a fast ripple was kept for analysis if it was visible only in the 250–600 Hz frequency range. The parameters listed above were selected through systematic data analysis and were found to produce results as good as those produced by a human operator. They had the advantage of standardizing the detection of oscillation events over all data sets, eliminating bias. The result was a list of "ripple events" and "fast ripples events" throughout the recording file, for each recorded region.

Detection of interictal spikes and of seizures

The same 10-min time periods selected for HFO analysis were also subjected to interictal spike detection. Interictal spikes were identified using custom-built routines in Matlab. Peaks crossing a threshold in SD above or below the background mean of the unfiltered local field potential were considered as potential interictal spikes. The threshold was adapted to each LFP signal in order to match what was found by visual analysis. Each detected event was visually examined to identify true interictal spikes and to exclude false positive events created by movement artefacts. We classified interictal spikes in three categories, based on the co-occurrence of HFOs in a 200 ms window before and after time 0, defined by the maximal peak after threshold crossing: (i) interictal spikes without HFOs, (ii) interictal spikes co-occurring with ripples, and (iii) interictal spikes co-occurring with fast ripples (Fig. 1). The incidence of these three types was expressed as rates (number of events per minute).

The end of the latent period and the beginning of the chronic period was based on the occurrence of the first spontaneous seizure, whether it was convulsive or non-convulsive. In order to assess the occurrence of seizures over time, LFPs recorded from all regions were analyzed, from the 4th to the 15th day after SE. Seizures were

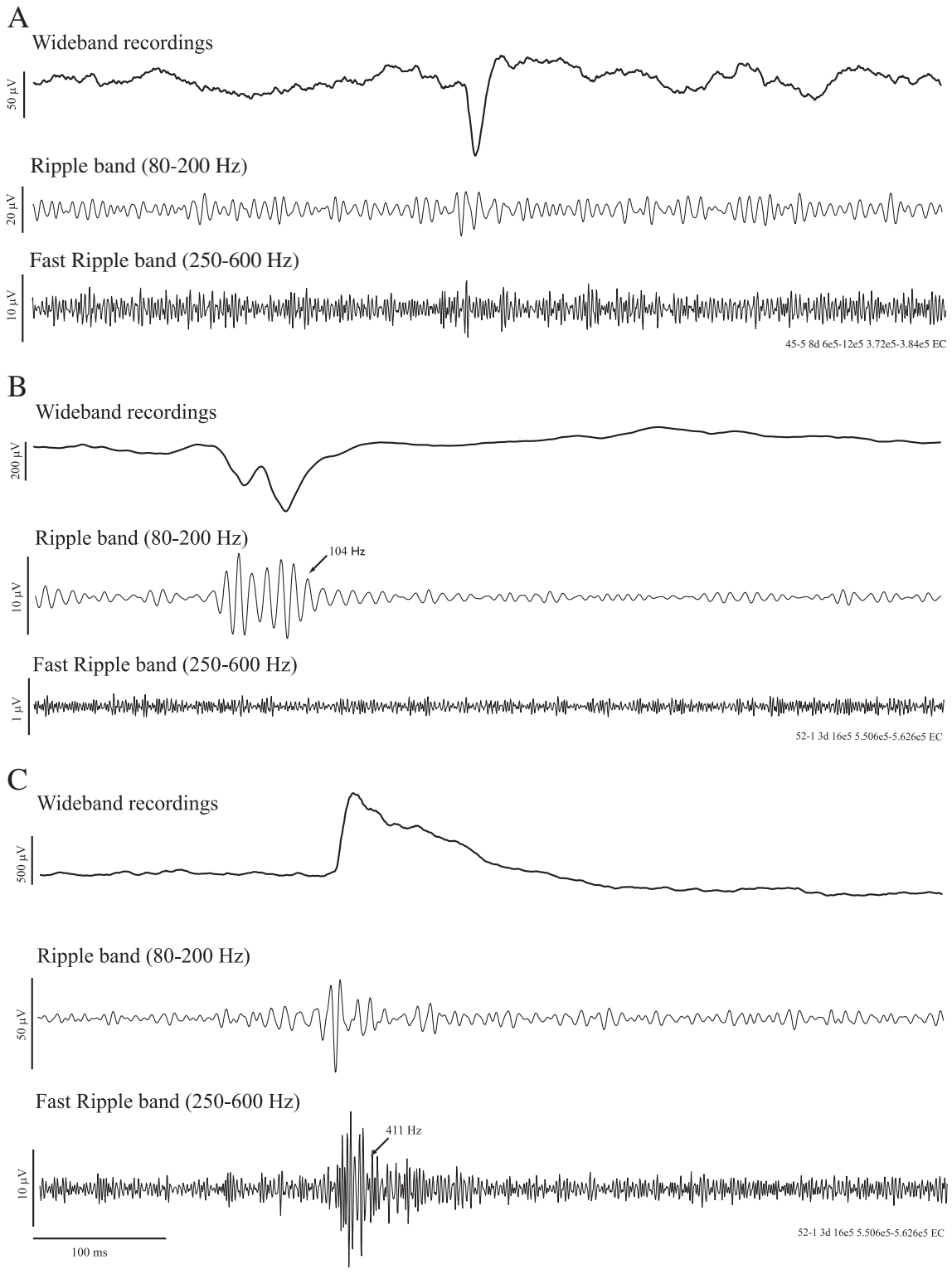

Fig. 1. LFP recordings from the EC in two rats showing interictal spikes with the occurrence of high frequency activity. A. LFP showing an interictal spike without high-frequency activity in the ripple and fast ripple band. B. interictal spike occurring with a ripple. C. interictal spike occurring with a fast ripple.

identified automatically with the ICTA-D seizure detector (Harmonie, Stellate, Canada). Validation of the results provided by the detector was performed by visual inspection of the LFP and the video. Seizures were classified as non-convulsive (stage 1–2 of the Racine's scale (1972) or convulsive (stage 3–5). Termination of convulsive seizures was usually followed by wet-dog shakes. On the LFP signal, seizures were characterised by ictal discharges of increasing amplitude that involved multiple channels, for a duration of at least 5 s. Seizure rate was defined as the number of seizures per day.

Statistical analysis

To prevent any effect of inter-individual variability, rates of interictal spikes with and without HFOs were transformed into Z-scores for each

rat, using the mean and SD of interictal spike rates from the 4th to the 15th day after SE. Normalized values obtained from all rats were then averaged for each day, from the 4th day to the 15th day after SE. Some recordings in some rats were not included due to bad electrode connection.

Variations of interictal spike rates over time

Significant changes in rates of interictal spikes with and without HFOs over time were assessed with repeated measures ANOVAs in Matlab (Trujillo-Ortiz et al., 2004). If a significant effect of time was observed ($p<0.05$), significant increases or decreases of interictal spike rates were identified by using a threshold obtained from the calculation of a 95% confidence interval, built around the average interictal spike rate from the 4th to the 15th day after SE. This analysis was performed because paired comparisons, normally used following a repeated measure ANOVA, were not relevant in the current context, in which we were trying to identify times with particularly low or high spiking rates. In order to study the overall evolution of interictal spike rates over time, correlations between interictal spike rates and days were performed using linear cross-correlation.

Interictal spike and seizure rates relationships

Stepwise linear regressions were performed in Matlab to test whether the rates of interictal spikes with and without HFOs are related to seizure occurrence. Stepwise linear regressions were also applied with seizure rates shifted back and forward in time. Significant linear regressions using seizure rates shifted back in time would indicate that interictal spike rates predict seizure occurrence, while significant linear regressions using forward shifted seizure rates would indicate that interictal spike rates are related to seizure occurrence recorded on the preceding day.

Variations of interical spike rates with region

Statistical analyses consisted of one-way ANOVAs with Scheffe pos-hoc tests to identify differences between anatomical sites when comparing the percentage of each category of interictal spikes recorded and their respective rate.

Results

Seizures and seizure clustering

We recorded a total of 144 spontaneous seizures between the 4th and the 15th day after SE from 7 rats. Animals presented with spontaneous seizures after a latent period of 6.1 ± 2.5 days. The onset of seizures was observed in the CA3 region in 71% of cases, while in the remaining cases no specific onset region could be identified. Fig. 2A illustrates a typical spontaneous seizure recorded 14 days after SE. The characteristic of these seizures were similar to those reported by us in a previous study (Bortel et al., 2010).

Seizures lasted on average 77.4 ± 35.2 s (Fig. 2C) and occurred at an average rate of 2.4 ± 1.7 per day (Fig. 2B); they usually occurred in clusters (more than 2 seizures per day) between the 9th and the 12th day after SE (Fig. 2B). Non-convulsive seizures (stage 1–2 of Racine scale) were first observed, followed by convulsive seizures (stage 3–5 of Racine scale) (Fig. 2D) (*cf.*, Bortel et al., 2010). Rates of non-convulsive and convulsive seizures were not significantly different when considering the average rates from the 4th to the 15th after SE (Fig. 2D, inset).

Interictal spikes

We recorded a total of 12,886 interictal spikes from 7 pilocarpine-treated animals. Rates of interictal spike rates varied significantly over time in every region (DG: $F=3.5$, $p<0.001$, EC : $F=2$, $p<0.05$, CA3: $F=6.5$, $p<0.001$, Sub: $F=2$, $p<0.05$). A marginally significant drop of interictal spike rates was observed in EC on the 13th day (Fig. 3B) and a marginally significant increase was observed in the subiculum on the 9th day (Fig. 3D). When considering the overall evolution of interictal spike rates over time, the DG was the only region to show a significant trend towards interictal spike rate increase over time ($r^2=0.7$, $p<0.05$) (Fig. 3A).

A linear regression analysis with seizure rates back shifted in time showed that interictal spike rates in the EC are the best predictors of seizure rates ($F=5.3$, $r^2=0.4$, $p<0.05$), suggesting a close relationship between interictal spike activity in this region and seizure occurrence on the following day (Fig. 3E). A linear regression analysis with seizure rates shifted forward in time did not produce any significant result. The overall rate of occurrence of interictal spikes did not vary with the anatomical site (Fig. 3F).

Interictal spikes without HFOs

Interictal spikes without HFOs ($n=10{,}096$) represented on average 74.1 ± 4.4% of all recorded interictal spikes. As seen for the total number of interictal spikes recorded, every region showed significant variations of interictal spike rates over time (DG: $F=2.8$, $p<0.005$, EC: $F=2.3$, $p<0.05$, CA3: $F=4.7$, $p<0.0001$, Sub: $F=2.8$, $p<0.01$). This was expected since interictal spikes without HFOs represented the majority of interictal spikes. The only significant decrease was observed in the EC on the 13th day after SE (Fig. 4B) and the subiculum showed again a marginally significant increase on the 9th day (Fig. 4D). Interictal spike rates without HFOs significantly increased over time in the DG ($r^2=0.7$, $p<0.05$) (Fig. 4A).

A linear regression analysis with seizure rates shifted back in time showed a significant relation between interictal spike activity without HFO and seizure occurrence in EC ($F=7.87$, $r^2=0.47$, $p<0.05$). More specifically, high rates of interictal spikes without HFOs were related to high seizure rates on the following day, suggesting that rates of interictal spikes without HFOs in this area can predict seizure occurrence on the following day (Fig. 4E). All regions showed similar percentages of interictal spikes without HFOs and rates were similar across regions (Figs. 4F, G).

Characteristics of HFOs

Fast ripple duration was significantly shorter than that of ripples ($p<0.001$) (Supplementary Fig. 2). Fast ripples could start at any moment during an interictal spike, but the highest probability of onset was before the peak of the interictal spike, (i.e., on its first phase) (Supplementary Fig. 3). The relationship between ripples and interictal spikes showed the same pattern. The onset of ripples mostly occurred during the spike component (Supplementary Fig. 4).

Interictal spikes with fast ripples

Five of 7 rats showed interictal spikes with fast ripples ($n=429$). On average, the first interictal spike with fast ripples was seen 5.8 ± 1.8 days after SE. Interictal spikes with fast ripples represented 4.9 ± 4.6% of all recorded interictal spikes. The majority (85.3%) of interictal spikes with fast ripples co-occurred with a single fast ripple, whereas 14.7% of them co-occurred with multiple fast ripples (not illustrated).

Temporal analysis of rates of interictal spikes with fast ripples revealed a significant effect of time in the EC ($F=3.1$, $p<0.005$), CA3 ($F=5.7$, $p<0.0001$) and subiculum ($F=2.8$, $p<0.01$). The EC showed marginally significant increases of rates of interictal spikes with fast

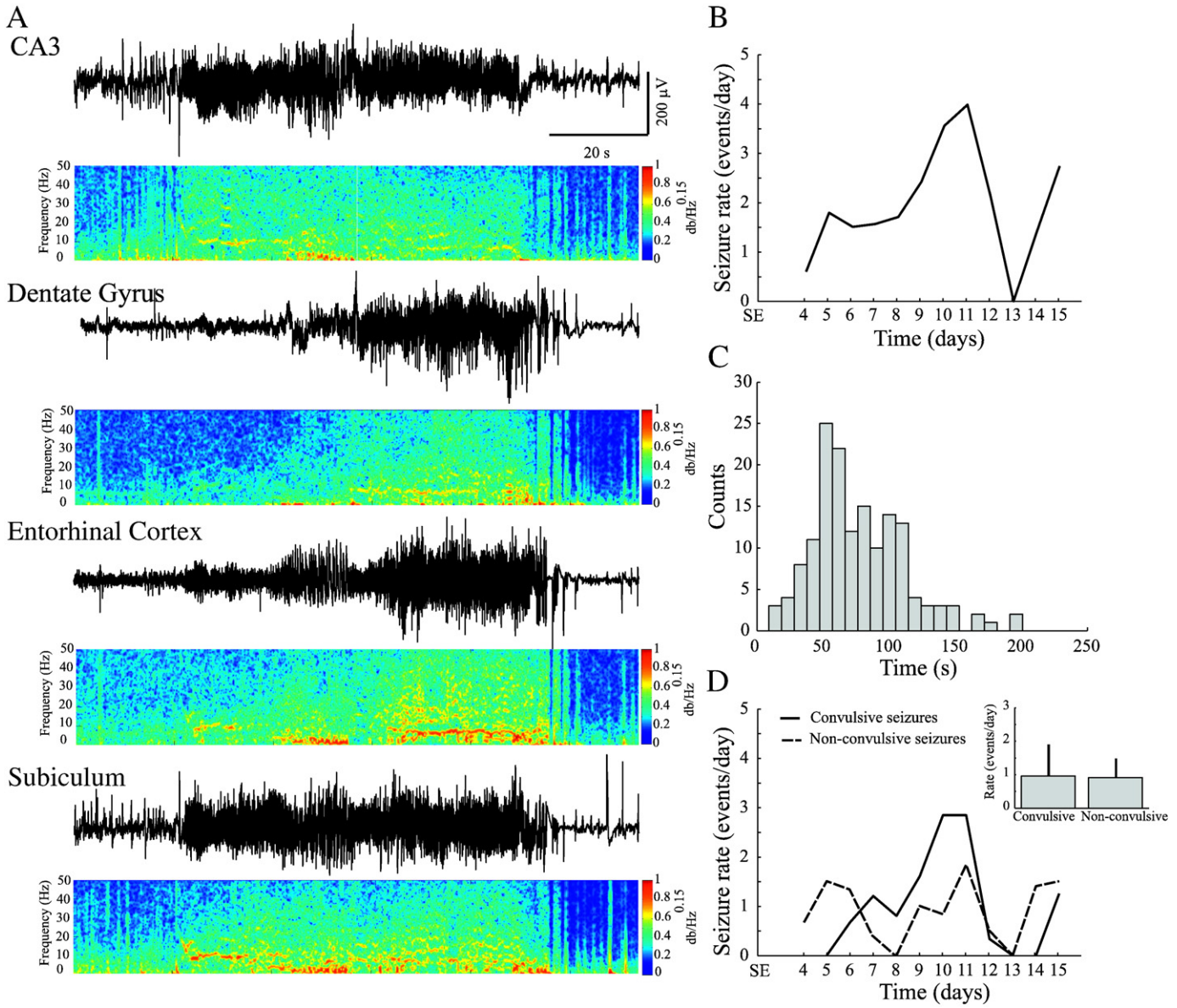

Fig. 2. A. a representative seizure recorded from multiple regions simultaneously. Power spectral densities (PSD) were obtained through a 4096-point Short-Time Fourier Transform, using time windows of 1 s with 75% overlap. The frequency band from 0 to 1000 Hz was normalized in amplitude from 0 to 1 and equalized with an exponential function with exponent 0.15, for better visualisation. B. average seizure rate for all rats, across the entire recording period (4 to 15 days after SE). Note that there is an increase of seizure rates between the 9th and the 12th day after SE. C. frequency distribution histogram of seizure duration. D. time graph showing the average rate of occurrence of convulsive and non-convulsive seizures. Note that non-convulsive seizures occurred before convulsive seizures. As shown in the inset, no significant difference was observed in their rate of occurrence.

ripples before and after the period of high seizure occurrence, on the 9th and 14th after SE (Fig. 5B). On the other hand, rates of interictal spikes with fast ripples started to increase in CA3 when seizure rates were also increasing, and reached a significantly high peak on the 11th day after SE (Fig. 5C).

A linear regression analysis also showed that rates of interictal spikes with fast ripples in CA3 were the best predictors of seizure rates ($F = 7.5$, $r^2 = 0.43$, $p < 0.05$), suggesting that interictal spike rates with fast ripples in this region reflect seizure occurrence (Fig. 5E). Finally, the subiculum showed a significant peak on the 12th day, which followed the day during which the peak of seizure rates was observed (Fig. 5D). A linear regression analysis with seizure rates shifted forward in time indeed showed a significant relationship between interictal spike rates with fast ripples in the subiculum and seizure activity ($F = 14.3$, $r^2 = 0.61$, $p < 0.005$), suggesting that interictal spike rates with fast ripples in this region reflect seizure occurrence recorded on the preceding day (Fig. 5F). The same analysis with seizure rates shifted backward in time did not show any significant relationships, indicating that interictal spike rates with fast ripples cannot be used to predict seizure occurrence on the following day. Both percentage and rate of interictal spikes with fast ripples did not vary significantly between regions (Figs. 5G, H).

Interictal spikes with ripples

A total of 1720 interictal spikes with ripples were recorded, representing $14.3 \pm 3.3\%$ of all recorded interictal spikes. Only 3.9% of interictal spikes with ripples co-occurred with multiple ripples (not illustrated). Activity in the ripple frequency range was recorded on average 4.6 ± 1.1 days after SE and was recorded in all rats. Repeated measures ANOVAs showed a significant effect of time in the DG ($F = 2.7$, $p < 0.01$), CA3 ($F = 3.2$, $p < 0.005$) and subiculum ($F = 4.4$, $p < 0.0005$). However, no significant increases or decreases of interictal spike rates were observed in these regions. In the EC, interictal

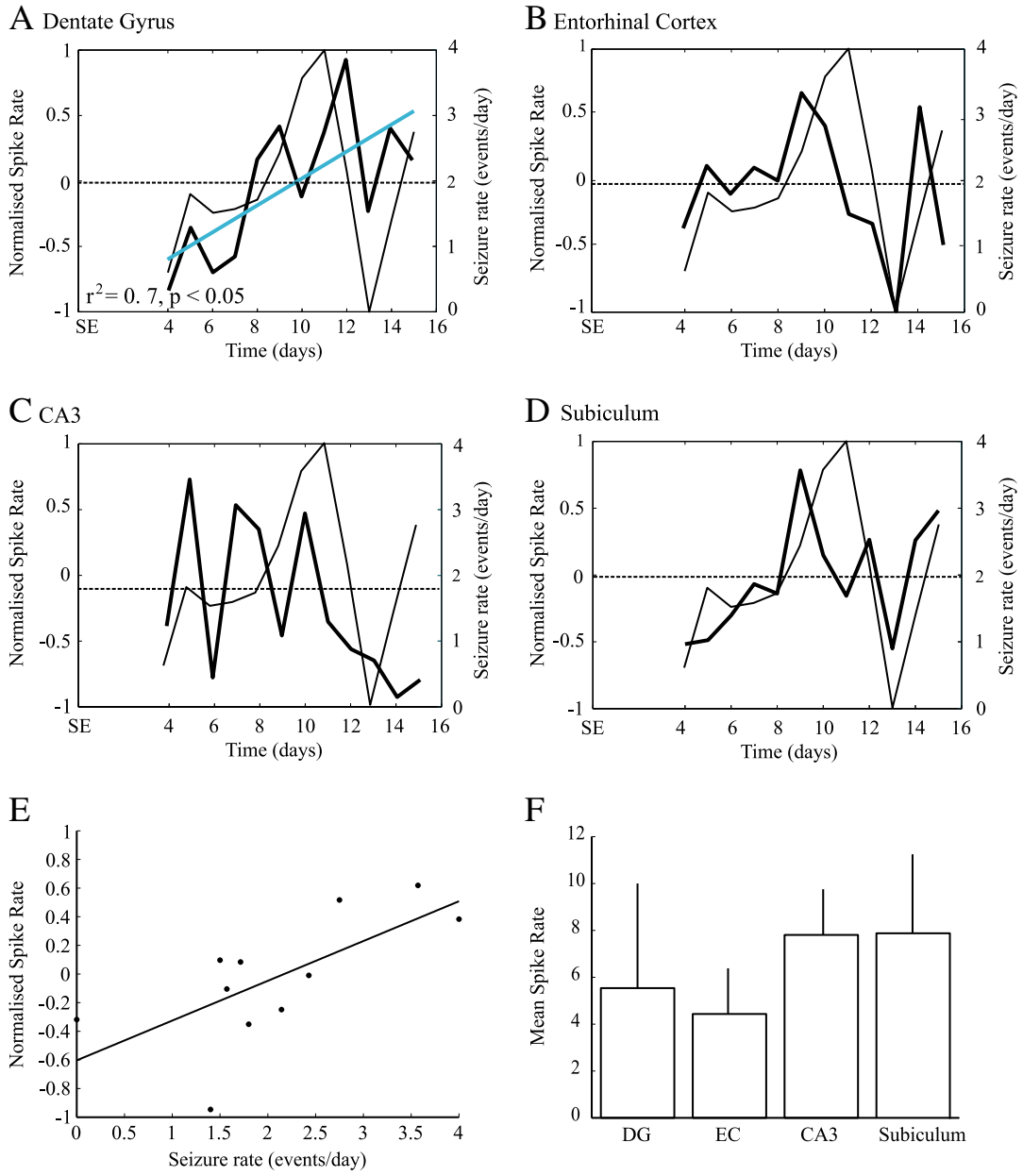

Fig. 3. Average rates of all recorded interictal spikes as obtained from DG (A), EC (B), CA3 (C) and subiculum (D). thick lines represent the normalized rates of interictal spikes (left y-axis), while thin lines represent seizure rates (right y-axis). The dashed line represents the average interictal spike rate, from the 4th to the 15th day after SE. The blue solid line indicates a significant trend of interictal spike rates over time in the DG (A). E. scatter plot showing a significant relation between rates of interictal spikes in the EC and seizure rates, suggesting that interictal spike rates in this region can be used as a predictor of seizure rates on the following day ($r^2 = 0.4$, $p < 0.05$). F. Average interictal spike rates from all recorded sites; no significant differences were observed.

spike rates decreased significantly over time ($r^2 = -0.6$, $p < 0.05$) (Fig. 6B). A similar and significant decrease was observed in CA3 ($r^2 = -0.7$, $p < 0.05$) (Fig. 6C). On the other hand, a significant increase of interictal spikes with ripples rates was seen over time in the DG ($r^2 = 0.6$, $p < 0.05$) (Fig. 6A). Linear regression analyses did not show any significant predictor variable of seizure rates. Both rate and percentage of interictal spikes with ripples did not significantly vary between regions (Figs. 6E and F).

Discussion

The main findings of our study can be summarized as follows. First, different categories of interictal spikes are recorded following pilocarpine-induced SE, and those not associated with HFOs represented the vast majority. Second, increases of rates of interictal spikes without HFOs in the EC predict upcoming periods of high seizure rates, while increases of rates of interictal spikes with fast ripples in the CA3 region occurred concomitantly with periods of seizure activity. Finally, rates of interictal spikes with ripples could not be used as predictors of seizure occurrence.

Rates of interictal spikes without HFOs

In all regions, there was a significant effect of time on the rates of interictal spikes without HFOs, although the only significant decrease was observed in the EC on the 13th day, when seizure rates reached minimal values. Rates of interictal spikes without HFOs in the EC were also predictors of seizure occurrence on the following day: low rates

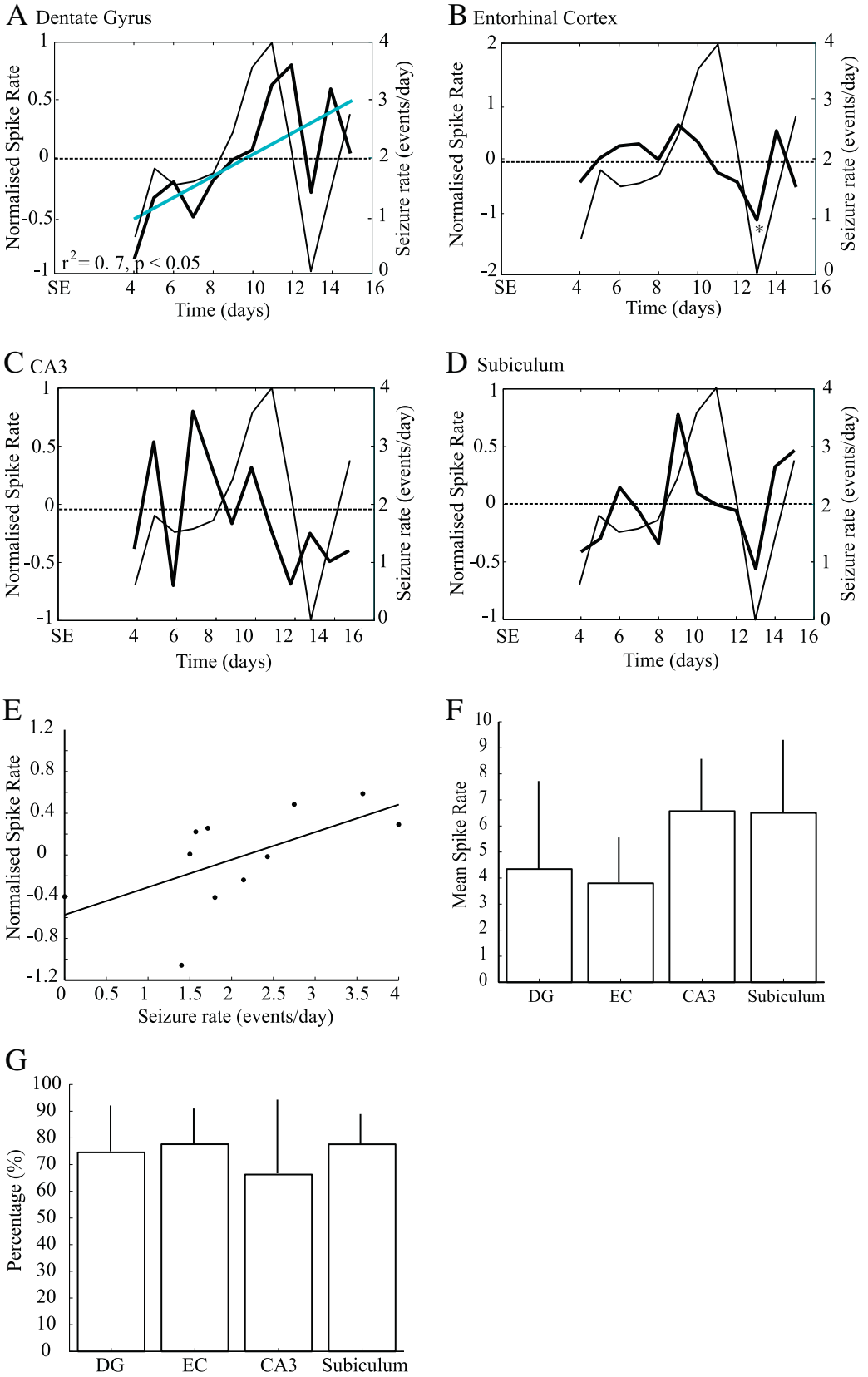

Fig. 4. A–D. Average rates of interictal spikes without HFOs. Note that the DG was the only region to show a significant increase of spike rates over time (A, blue line). A significant decrease of interictal spike rates was observed in the EC (B), on the 13th day (*). E. scatter plot showing that rates of interictal spikes without HFOs in the EC are predictors of seizure rates on the following day. Bar graphs showing the average rate (E) and percentage (F) of interictal spikes without HFOs in each region. No significant difference were observed.

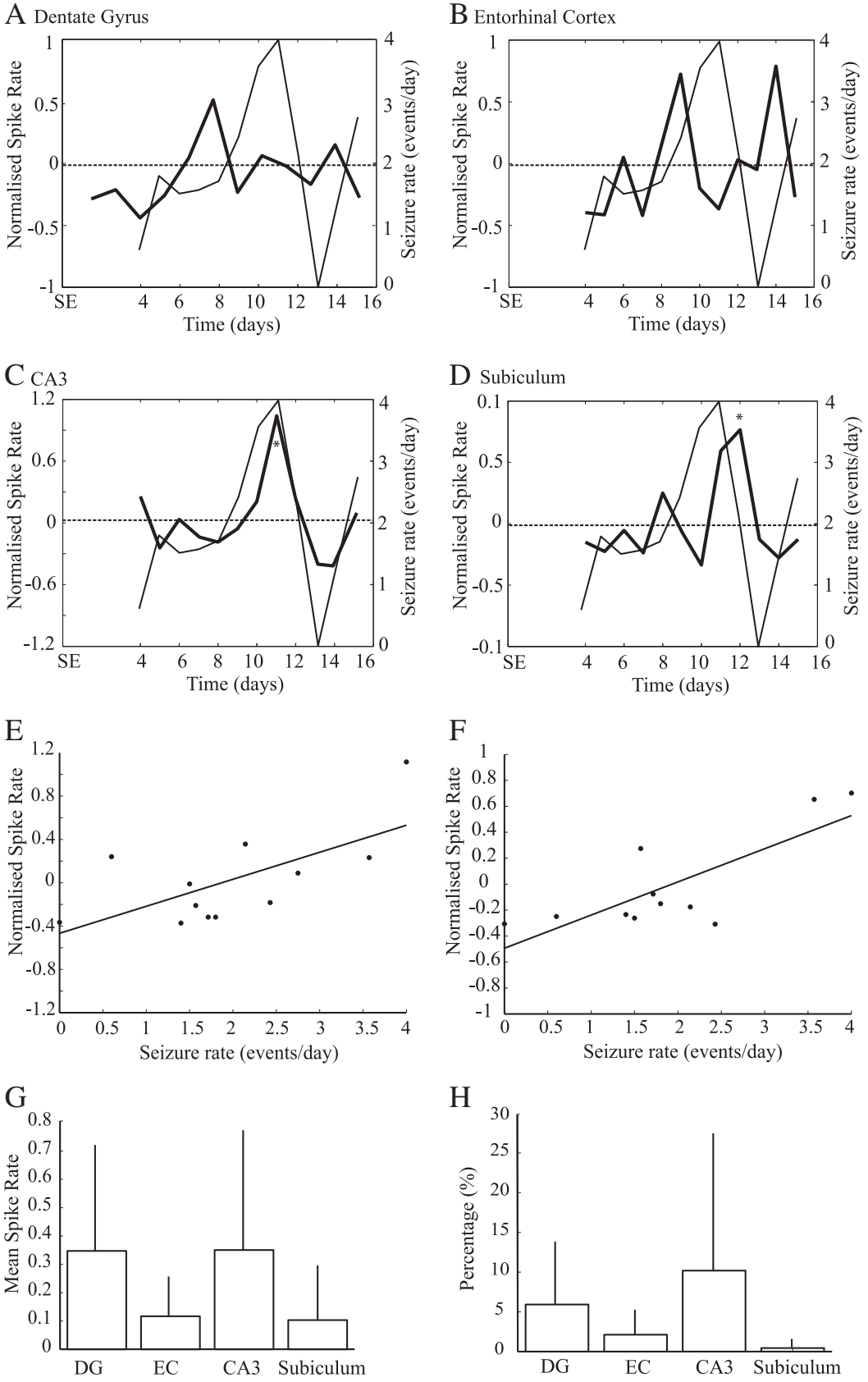

Fig. 5. A–D. average rates of interictal spikes that co-occurred with fast ripples. A significant increase of interictal spike rates was observed on the 11th day in CA3 (C) and on the 12th day in the subiculum (D). E. scatter plot showing that interictal spike rates in CA3 are related to seizure occurrence. F. scatter plot showing a significant relation between interictal spike rates in the subiculum and seizure rates recorded on the preceding day. There was no significant differences between anatomical sites, when comparing the rate (G) and the percentage (H) of interictal spikes with fast ripples recorded in each region.

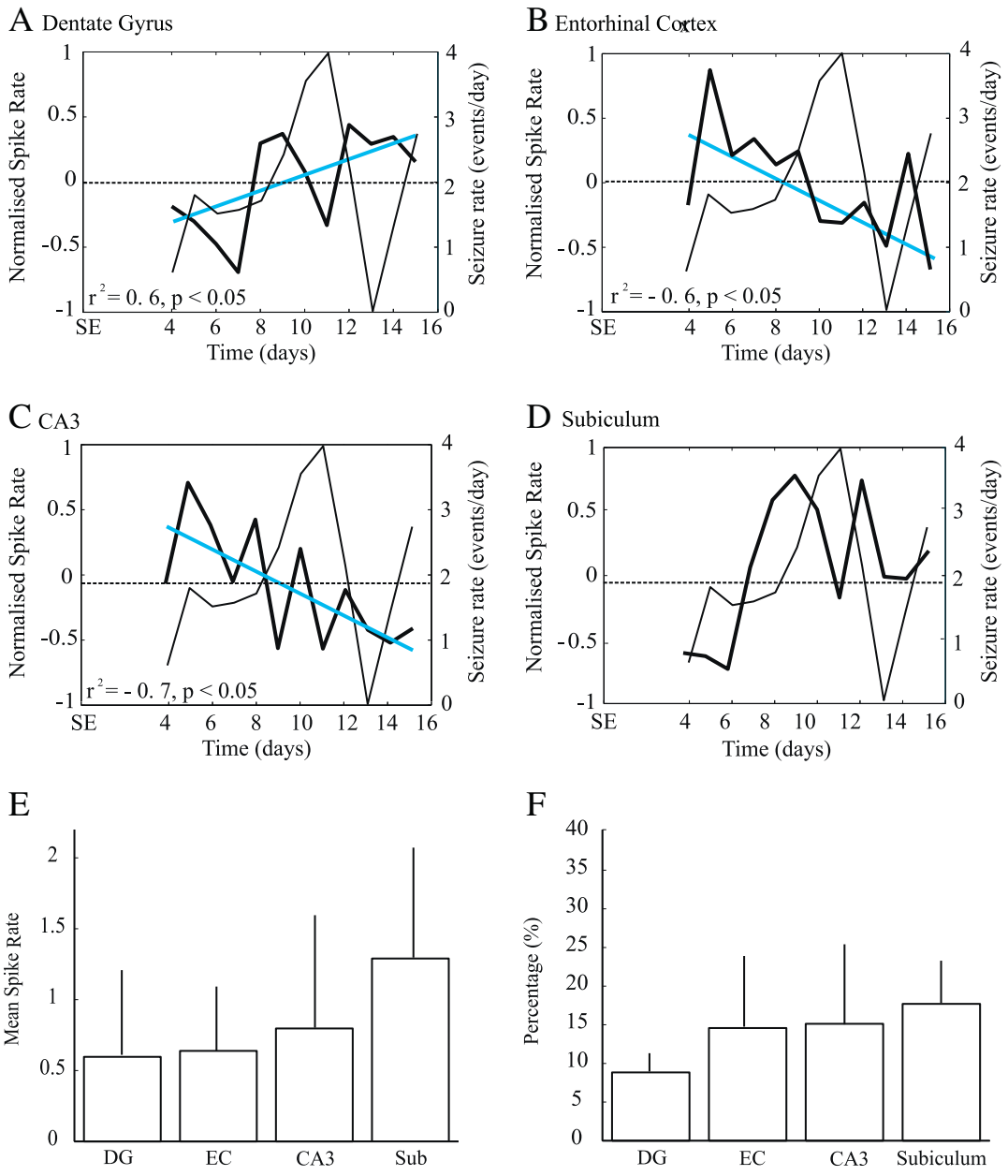

Fig. 6. A–D. Average rates of interictal spikes that co-occurred with ripples. The DG (A, blue line) showed a significant increase of rates of interictal spikes with ripples over time, while the EC (B) and CA3 region (C) showed significant decreases. There was no significant differences between anatomical sites, when comparing the percentage and the rate of interictal spikes with ripples recorded in each region (E,F).

of interictal spikes without HFOs in the EC were followed on the next day by low seizure rates, while high rates of interictal activity predicted high seizure rates. As one of the main inputs to the hippocampus, the EC may promote epileptogenesis in other downstream regions, because of its high susceptibility to become hyperexcitable following SE (Bragin et al., 2009; de Guzman et al., 2008). *In vitro* studies have shown that slices obtained from pilocarpine-treated animals generate epileptiform discharges that originate from the EC and suggested that this region may contribute to the generation and propagation of seizure across the limbic system, through a decreased control of EC excitability by hippocampal outputs (Avoli et al., 2002; D'Antuono et al., 2002; Panuccio et al., 2010; Wozny et al., 2005). Our finding of a significant relation between interictal activity and seizure occurrence in the EC supports the hypothesis conceiving this region as one of the primary site where TLE develops. Changes in interictal activity in this region may be involved in seizure generation.

Relationship between spike and HFOs

HFOs were mainly observed during the first phase of the interictal spike, and they rarely occurred during the slow-wave. This is in line with previous studies performed in patients and suggests that HFOs are generated during the spike (Jacobs et al., 2008; Urrestarazu et al., 2007). Since interictal spikes are believed to represent the summated post-synaptic potentials generated by hypersynchronous neurons (Johnston and Brown, 1981), our results supports the view that HFOs may represent the summated activity of synchronously discharging neurons (Engel et al., 2009).

Interictal spikes with fast ripples

A significant increase of fast ripple activity in the CA3 region was observed during the period of high seizure rates, on the 11th day.

Therefore, fast ripple activity in this region could reflect susceptibility to seizure occurrence and seizure clustering. Our data also indicate that fast ripples are more tightly linked to high seizure rates in the seizure onset zone, a finding that is in line with previous studies (Bragin et al., 2002b; Jacobs et al., 2008; Staba et al., 2007). They also suggest that increases in rates of interictal spikes with fast ripples in the seizure onset zone may be useful to identify periods of increased seizure occurrence (Frei et al., 2010).

The rates of interictal spikes with fast ripples in the EC and CA3 showed inverted patterns of evolution (see Fig. 5B, C). Increases of fast ripple activity in CA3 (from day 10 to day 12) occurred simultaneously to decreases in EC. Similarly, increases of rates of interictal spikes with fast ripples occurred in the EC (from day 8 to day 10 and from day 13 to day 15) while rates were low in CA3. These data are in line with previous *in vitro* studies, in which it was proposed that CA3-driven interictal activity controls the EC propensity to generate ictal discharges (Barbarosie and Avoli, 1997; Barbarosie et al., 2002). Cell damage and synaptic reorganization in CA3 that is seen following pilocarpine treatment (Biagini et al., 2008; Cavalheiro et al., 1996; Turski et al., 1984) may in fact reduce hippocampal output activity and thus release the control exerted on the EC (D'Antuono et al., 2002; Panuccio et al., 2010). The increased rates of interictal spikes with fast ripples in CA3 during seizure clustering could represent the attempt of CA3 to control the EC propensity to promote ictogenesis. However, another possible explanation for the increase of interictal spikes with fast ripples in CA3 only during periods of high seizure rates could rest on the fact that this region is extensively damaged following SE. Early and widespread neuronal loss in CA3 may thus prevent the generation of HFOs, until the network reorganizes itself many days after the SE. Indeed, the CA3 region presents with extensive cell damage following pilocarpine treatment (Biagini et al., 2008; Mello et al., 1993, Mello and Covolan 1996) and some studies have shown a close relationship between fast ripple rates and neuronal loss in this region (Foffani et al., 2007).

The increase of fast ripple activity in the subiculum after the period of seizure clustering suggests the involvement of this limbic area in the epileptogenic process. Several *in vitro* studies have demonstrated that the subiculum plays a pivotal role in the pilocarpine model of temporal lobe epilepsy, and in the human condition (de Guzman et al., 2006; Knopp et al., 2005; Vreugdenhil et al., 2004; Wellmer et al., 2002). *Ex vivo* experiments have also shown increased expression of FosB/ΔFosB in the subiculum of pilocarpine-treated rats (Biagini et al., 2005). Increased subicular activity may thus amplify hippocampal outputs which would in turn sustain parahippocampal ictal activity and epileptogenesis.

Another finding in our study is that even though all rats developed seizures, only 5 of them showed fast ripple activity. These results are in agreement with those of Bragin et al. (2004), and reinforce the idea that fast ripples may not be a prerequisite for spontaneous seizure occurrence. However, the absence of fast ripple activity in two animals could also be due to the use of fixed electrodes that may have compromised our ability to record fast ripples. Fast ripples, at variance with ripples, are generated by spatially localized, small neuronal networks (Chrobak and Buzsáki, 1996); hence our ability to record fast ripples might have been higher if we would have used moveable electrodes (Bragin et al., 2002a).

Interictal spikes with ripples

Interictal spikes with ripples were recorded earlier than those with fast ripples following the initial SE. This phenomenon was observed in the EC, as well as in the CA3 region (although increases of ripple activity did not reach significance). However, interictal spikes with ripples did not appear as reliable markers of epileptogenesis as it was observed for fast ripples, as rates significantly decreased over time in the EC and CA3 region. In the subiculum, no specific pattern was observed. These results indicates that ripples cannot be recorded for long time periods in these regions or that fast ripple activity is gradually replacing ripple activity. However, to firmly establish whether ripples are gradually replaced by fast ripple activity, we would need recording periods that extends to more than 15 days. On the other hand, we have observed a significant increase of ripple rates over time in the DG. Since ripples are not observed in this region under normal conditions, the occurrence of this type of activity could suggest that an epileptogenic process is gradually developing there.

Conclusion

Our findings suggest that the spatial distribution and temporal development of interictal spikes depend on their co-occurrence with high-frequency activity. Interictal spikes without HFOs and with high-frequency activity may thus reflect different dynamic processes underlying epileptogenesis. Indeed, rates of interictal spikes without HFOs in the EC could be used to predict high susceptibility to seizures on the following days. On the other hand, interictal spikes with fast ripples in the seizure onset zone (which was frequently identified in the CA3 area) may be used to identify periods of increased seizure occurrence. Increase of fast ripple activity may thus provide a time window during which regions of the temporal lobe undergo meaningful changes in neural excitability.

Many questions related to HFOs remain unanswered, especially on the role of high-frequency activity in spontaneous seizure generation, and on the physiological substrate of HFOs. Our study, however, addresses an important point on the developmental and spatial distribution patterns of HFOs, since it provides information that may guide future mechanistic studies on these events. We also document the activity of different types of interictal spikes, depending on their co-occurrence with different HFOs. We are confident that the results reported here will be important for future investigations on interictal activity, as different interictal spikes may be associated with distinct pathological neuronal states that may sustain epileptogenesis.

Supplementary materials related to this article can be found online at doi:10.1016/j.nbd.2011.01.007.

Acknowledgments

This study was supported by the Canadian Institutes of Health Research (CIHR grants 8109 and 102710) and the Savoy Foundation. We are grateful to Dr. R. Courtemanche and J. Robinson for providing help with histology, and to Dr. G. Panuccio for helpful comments on an earlier version of the manuscript. We also thank J.-P. Acco for the artwork.

None of the authors has any conflict of interest to disclose.

References

Avoli, M., D'Antuono, M., Louvel, J., Kohling, R., Biagini, G., D'Arcangelo, G., Tancredi, V., 2002. Network and pharmacological mechanisms leading to epileptiform synchronization in the limbic system in vitro. Prog. Neurobiol. 68, 167–207.

Bagshaw, A.P., Jacobs, J., LeVan, P., Dubeau, F., Gotman, J., 2009. Effect of sleep stage on interictal high-frequency oscillations recorded from depth macroelecrodes in patients with focal epilepsy. Epilepsia 50, 617–628.

Barbarosie, M., Louvel, J., D'Antuono, M., Kurcewicz, I., Avoli, M., 2002. Masking synchronous GABA-mediated potentials controls limbic seizures. Epilepsia 43, 1469–1479.

Barbarosie, M., Avoli, M., 1997. CA3-driven hippocampal-entorhinal loop controls rather than sustains in vitro limbic seizures. J. Neurosci. 17, 9308–9314.

Biagini, G., Baldelli, E., Longo, D., Contri, M.B., Guerrini, U., Sironi, L., Gelosa, P., Zini, I., Ragsdale, D.S., Avoli, M., 2008. Proepileptic influence of a focal vascular lesion affecting entorhinal cortex-CA3 connections after status epilepticus. J. Neuropathol. Exp. Neurol. 67, 687–701.

Biagini, G., D'Archangelo, E., Baldelli, M., D'Antuono, V., Tancredi, V., Avoli, M., 2005. Impaired activation of CA3 pyramidal neuronsin the epileptic hippocampus. Neuromol. med. 7, 325–342.

Bortel, A., Lévesque, M., Biagini, G., Gotman, J., Avoli, M., 2010. Convulsive status epilepticus duration as determinant for epileptogenesis and interictal discharge generation in the rat limbic system. Neurobiol. Dis. 40, 478–489.

Bragin, A., Wilson, C.L., Almajano, J., Mody, I., Engel, J., 2004. High-frequency oscillations after status epilepticus : epileptogenesis and seizure genesis. Epilepsia 45, 1017–1023.
Bragin, A., Engel, J., Wilson, C.L., Vizentin, E., Mathern, G.W., 1999. Electrophysiological analysis of a chronic seizure model after unilateral hippocampal KA injection. Epilepsia 40, 1210–1221.
Bragin, A., Mody, I., Wilson, C.L., Engel, J., 2002a. Local generation of fast ripples in epileptic brain. J. Neurosci. 22, 2012–2021.
Bragin, A., Wilson, C.L., Engel, J., 2000. Chronic epileptogenesis requires development of a network pathologically interconnected neuron clusters: a hypothesis. Epilepsia 41 (S6), S144–S152.
Bragin, A., Wilson, C.L., Engel, J., 2003. Spatial stability over time of brain areas generating fast ripples in the epileptic rat. Epilepsia 44, 1233–1237.
Bragin, A., Wilson, C.L., Engel, J., 2007. Voltage depth profiles of high-frequency oscillations after kainic acid-induced status epilepticus. Epilepsia 48 (S5), 35–40.
Bragin, A., Wilson, C.L., Staba, R.J., Reddick, M.S., Fried, I., Engel, J., 2002b. Interictal high frequency oscillations (80–500 Hz) in the human epileptic brain: entorhinal cortex. Ann. Neurol. 52, 407–415.
Bragin, D.E., Sanderson, J.L., Peterson, S., Connor, J.A., Muller, W.S., 2009. Development of epileptiform excitability in the deep entorhinal cortex after status epilepticus. Eur. J. Neurosci. 30, 611–624.
Cavalheiro, E.A., Santos, N.F., Priel, M.R., 1996. The pilocarpine model of epilepsy in mice. Epilepsia 37, 1015–1019.
Chrobak, J.J., Buzsáki, G., 1996. High-frequency oscillations in the output networks of the hippocampal entorhinal axis of the freely behaving rat. J. Neurosci. 16, 3056–3066.
Crépon, B., Navarro, V., Hasboun, D., Clemenceau, S., Martinerie, J., Baulac, M., Adam, C., Le Van Quyen, M., 2010. Mapping interictal oscillations greater than 200 Hz recorded with intracranial macroelectrodes in human epilepsy. Brain 133, 33–45.
D'Antuono, M., Benini, R., Biagini, G., D'Arcangelo, G., Barbarosie, M., Tancredi, V., Avoli, M., 2002. Limbic network interactions leading to hyperexcitability in a model of temporal lobe epilepsy. J. Neurophysiol. 87, 634–639.
de Guzman, P., Inaba, Y., Baldelli, E., de Curtis, M., Biagini, A., Avoli, M., 2008. Network hyperexcitability within the deep layers of the pilocarpine-treated rat entorhinal cortex. J. Physiol. 586, 1867–1883.
de Guzman, P., Inaba, Y., Biagini, G., Baldelli, E., Mollinari, C., Merlo, D., Avoli, M., 2006. Subiculum network excitability is increased in a rodent model of temporal lobe epilepsy. Hippocampus 16, 843–860.
Engel, J., Bragin, A., Staba, R., Mody, I., 2009. High-frequency oscillations: what is normal and what is not? Epilepsia 50, 598–604.
Foffani, G., Uzcategui, Y.G., Gal, B., Menendez de la Prida, L., 2007. Reduced spike-timing reliability correlates with the emergence of fast ripples in the rat epileptic hippocampus. Neuron 55, 930–941.
Frei, M.G., Zaveri, H.P., Arthurs, S., Bergey, G.K., Jouny, C.C., Lehnertz, K., Gotman, J., Osorio, I., Netoff, T., Freeman, W.J., Jefferys, J., Worrell, G., Le Van Quyen, M., Schiff, S.J., Mormann, F., 2010. Controversies in epilepsy: debates held during the Fourth International Workshop on Seizure Prediction. Epilepsy Behav. 19, 4–16.
Jacobs, J., LeVan, P., Chander, R., Hall, J., Dubeau, F., Gotman, J., 2008. Interictal high-frequency oscillations (80–500 Hz) are an indicator of seizure onset areas independent of spikes in the human epileptic brain. Epilepsia 49, 1893–1907.
Jacobs, J., LeVan, P., Châtillon, C.E., Olivier, A., Dubeau, F., Gotman, J., 2009. High frequency oscillations in intracranial EEGs mark epileptogenicity rather than lesion type. Brain 132, 1022–1037.
Johnston, D., Brown, T.H., 1981. Giant synaptic potential hypothesis for epileptiform activity. Science 211, 294–297.
Knopp, A., Kivi, A., Heinemann, U., Behr, J., 2005. Cellular and network properties of the subiculum in the pilocarpine model of temporal lobe epilepsy. J. Comp. Neurol. 483, 476–488.
Martin, B.S., Kapur, J., 2008. A combination of ketamine and diazepam synergistically controls refractory status epilepticus induced by cholinergic stimulation. Epilepsia 49, 248–255.
Mello, L.E., Cavallheiro, E.A., Tan, A.M., Kupfer, W.R., Pretorius, J.K., 1993. BabbTL, Finch DM. Circuit mechanisms of seizures in the pilocarpine model of chronic epilepsy: cell loss and mossy fiber sprouting. Epilepsia 34, 985–995.
Mello, L.E., Covolan, L., 1996. Spontaneous seizures preferentially injure interneurons in the pilocarpine model of chronic spontaneous seizures. Epilepsy Res. 26, 123–129.
Panuccio, G., D'Antuono, M., de Guzman, P., De Lannoy, L., Biagini, G., Avoli, M., 2010. In vitro ictogenesis and parahippocampal networks in a rodent model of temporal lobe epilepsy. Neurobiol. Dis. 39, 372–380.
Paxinos, G., Watson, C., 1998. The rat brain in stereotaxic coordinates, Fourth Edition. Academic Press, San Diego.
Racine, R.J., 1972. Modification of seizure activity by electrical stimulation. II. Motor seizure,. Electroencephalography and Clinical Neurophysiol. 32, 281–294.
Schevon, C.A., Trevelyan, A.J., Schroeder, C.E., Goodman, R.R., McKhann Jr., G., Emerson, R.G., 2009. Spatial characterization of interictal high frequency oscillations in epileptic neocortex. Brain 132, 3047–3059.
Staba, R.J., Frighetto, L., Behnke, E.J., Mathern, G.W., Field, S., Bragin, A., Ogren, J., Fried, I., Wilson, C.L., Engel, J., 2007. Increased fast ripple to ripple ratios correlate with reduced hippocampal volumes and neuron loss in temporal lobe epilepsy patients. Epilepsia 48, 2130–2138.
Staba, R.J., Wilson, C.L., Bragin, A., Jhung, D., Fried, I., Engel, J., 2004. High-frequency oscillations recorded in human medial temporal lobe during sleep. Ann. Neurol. 56, 108–115.
Trujillo-Ortiz, A., Hernandez-Walls, R., Trujillo-Perez, R.A., 2004. RMAOV1 : One-way repeated measures ANOVA. A Matlab file[WWW document]. URL http://www.mathworks.com/matlabcentral/filexchange/loadFile.do?objectId=5576.
Turski, W.A., Cavalheiro, E.A., Bortolotto, Z.A., Mello, L.M., Schwarz, M., Turski, L., 1984. Seizures produced by pilocarpine in mice: a behavioural, electroencephalographic, and morphological analysis. Brain Res. 12, 237–253.
Urrestarazu, E., Chander, R., Dubeau, F., Gotman, J., 2007. Interictal high-frequency oscillations (100–500 Hz) in the intracerebral EEG of epileptic patients. Brain 130, 2354–2366.
Vreugdenhil, M., Hoogland, G., van Veelen, C.W., Wadman, W.J., 2004. Persistent sodium current in subicular neurons isolated from patients with temporal lobe epilepsy. Eur. J. Neurosci. 19, 2769–2778.
Wellmer, J., Su, H., Beck, H., Yaari, Y., 2002. Long-lasting modification of intrinsic discharge properties in subicular neurons following status epilepticus. Eur. J. Neurosci. 16, 259–266.
Wozny, C., Gabriel, S., Jandova, K., Schulze, K., Heinemann, U., Behr, J., 2005. Entorhinal cortex entrains epileptiform activity in CA1 in pilocarpine treated-rats. Neurobiol. Dis. 19, 451–460.
Ziljmans, M., Jacobs, J., Zelmann, R., Dubeau, F., Gotman, J., 2009. High frequency oscillations and seizure frequency in patients with focal epilepsy. Epilepsy Res. 85, 287–292.